# Timing Excitation and Inhibition in the Cortical Network

**Albert Compte, Ramon Reig, and Maria V. Sanchez-Vives**

**Abstract** The interaction between excitation and inhibition in the cerebral cortex network determines the emergent patterns of activity. Here we analyze the specific engagement of excitation and inhibition during a physiological network function such as slow oscillatory activity (<1 Hz), during which up and down cortical states alternate. This slow rhythm represents a well-characterized physiological activity with a range of experimental models from in vitro maintained cortical slices to sleeping animals. Excitatory and inhibitory events impinging on individual neurons were identified during up and down network states, which were recognized by the population activity. The accumulation of excitatory and inhibitory events at the beginning of up states was remarkably synchronized in the cortex both in vitro and in vivo. The same synchronization prevailed during the transition from up to down states. The absolute number of detected synaptic events pointed as well towards a delicate balance between excitation and inhibition in the network. The mechanistic and connectivity rules that can support these experimental findings are explored using a biologically inspired computer model of the cortical network.

## Excitation and Inhibition During Cortical Up and Down States

Basal excitability and recurrent connectivity in the cerebral cortical network [18, 22] induce neuronal firing that reverberates in the circuit, resulting in an emergent network activity. During slow-wave sleep and anesthesia, this activity is organized in the cerebral cortex network in a slow (<1 Hz) rhythmic pattern consisting of interspersed up (or activated) and down (or silent) states (Fig. 1) [21, 41, 44]. This rhythm is recorded in the thalamocortical loop, but persists in the cortex following thalamectomy [42]. Furthermore, it can be generated in cortical slices maintained

M.V. Sanchez-Vives (✉)
Institut d'Investigacions Biomèdiques August Pi i Sunyer (IDIBAPS), 08036 Barcelona, Spain
Institució Catalana de Recerca i Estudis Avançats (ICREA), 08036 Barcelona, Spain
e-mail: msanche3@clinic.ub.es

K. Josić et al. (eds.), *Coherent Behavior in Neuronal Networks*, Springer Series in Computational Neuroscience 3, DOI 10.1007/978-1-4419-0389-1_2,

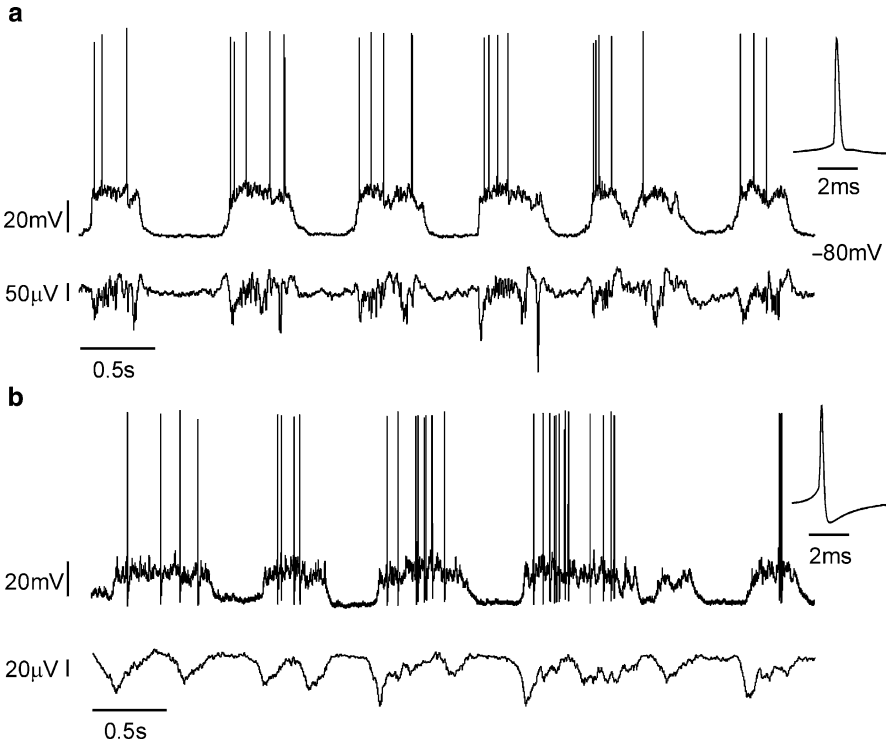


**Fig. 1** Slow rhythmic activity in excitatory and inhibitory neurons in vivo. (**a**) Successive up states recorded intracellularly from a regular spiking neuron in vivo (*top trace*). Inset illustrates an averaged action potential. Local field potential in the close vicinity (ca 100 μm) reflects network activity (*bottom trace*). (**b**) Successive up states recorded intracellularly from a fast spiking neuron in vivo (*top trace*). Note the higher firing frequency during up states displayed by the fast spiking neuron. Averaged action potential is represented in the inset. Local field potential from the vicinity in the *bottom trace*

in vitro [35], bearing a remarkable similarity to cortical activity during slow-wave sleep or anesthesia. Spontaneous slow rhythmic activity can also be recorded from disconnected cortical slabs in vivo [47]. Therefore, the slow rhythm is generated in the local cortical network, although the thalamic network can generate a similar rhythm if activated by metabotropic glutamate receptors [52].

The understanding of the detailed cellular and network mechanisms that regulate the aforementioned emergent activity provides a valuable insight into cortical function, and more generally into properties and regulation in neuronal networks. A key element in the balance and control of either spontaneous emergent or evoked cortical activity is the relation between excitation and inhibition. Slow oscillatory activity represents a well-characterized physiological activity with a range of experimental models, from in vitro to sleeping animals, where the specific engagement of excitation and inhibition in physiological network function can be studied. This

chapter will be devoted to excitatory and inhibitory activation during the occurrence of up and down spontaneous cortical states both in the real and in a modeled cortical network. The purpose is to understand how the network properties are tuned to achieve functional equilibrium and how this equilibrium can be eventually lost, as for instance in epilepsy. The approach we will present is both experimental and theoretical. In the experiments, we measure the time of occurrence of excitatory and inhibitory synaptic potentials during network activity. In the computational model, the relationship between structural parameters of network connectivity and the timing of excitatory and inhibitory inputs is explored.

The activated periods during rhythmic activity, or up states, are periods of intense synaptic activity that generate neuronal firing by pushing neuronal membrane potential above firing threshold. Both excitatory and inhibitory neurons fire during up states, while they remain relatively silent during down states. Several lines of evidence confirm that both types of neurons fire during up states (Fig. 1). From the first studies oscillations [41] it was already reported that not only excitatory electrophysiological types but also inhibitory also inhibitory ones (fast spiking neurons) fired during up states. membrane potential to different values by means of current injection further illustrated the coexistence of both excitatory and inhibitory potentials during up states in vivo and in vitro (Fig. 2) [35, 41]. Indeed, practically every recorded neuron participated in the rhythm with enhanced firing during the up state [7, 8, 35, 41, 43]. Quantification in striatal neurons also confirmed the participation of both excitatory and inhibitory events during participation of both excitatory and inhibitory events during Although all this evidence supports the simultaneous activation of Although all this evidence supports the simultaneous activation of oscillation, the issue of the timing of both types of events remains unsettled. A computational model of propagating slow oscillations predicted that inhibitory neurons should activate to their maximal rate slightly ahead in time than neighboring pyramidal neurons at the beginning of the up states pyramidal neurons at the beginning of the up states that this could be supported experimentally, although the trend did not reach statistical significance [17]. At the end of the up state, instead, experiments in vivo indicate that excitatory firing outlasts inhibitory firing [17].

So far, most studies have analyzed the relative contribution of excitation and inhibition to the conductance changes that neurons experience in the course of network activity [1,4,17,29,30,34,38]. A related aspect that has received much less attention is how the timing of excitatory and inhibitory events contributes to the excitation-inhibition balance [6]. Conductance measurements during up states reveal that the weight of excitation and inhibition is well balanced in vivo [17], and similarly in vitro [38], as also argued theoretically [5]. Still, there are some contradictory findings reported in the literature. Conductance measurements suggest that excitatory conductance dominates slightly at the beginning and the end of the up states but is otherwise comparable to inhibitory conductance [17]. Other studies, instead, report that the inhibitory conductance is much larger during up states [34].

The general understanding achieved by different methods is that excitation and inhibition balance each other, and this has been reported both during spontaneous or sensory activated cortical activity [1, 17, 27, 29, 37–39, 51]. However, we do not

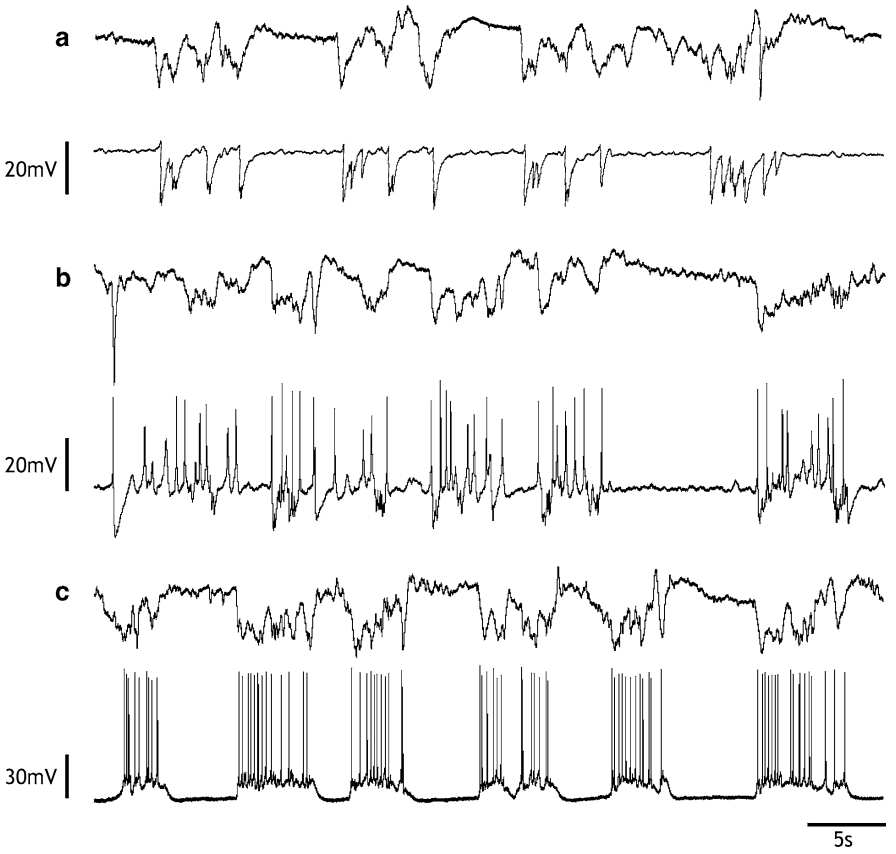


**Fig. 2** Excitatory and inhibitory synaptic potentials during slow oscillations in the auditory cortex *in vivo*. In the three panels (A, B and C) the unfiltered local field potential on top and intracellular recordings at the bottom. (**a**) Intracellular membrane potential at −15 mV to illustrate the IPSPs occurring during the up states. Sodium action potentials have been inactivated by depolarization. (**b**) Intracellular membrane potential at −45 mV illustrates a mix of IPSPs and EPSPs, while sodium action potentials are partially inactivated by depolarization. (**c**) Intracellular membrane potential at −75 mV illustrating suprathreshold up states. All intracellular recordings are from the same neuron

know exactly how this balance is achieved in terms of the contrasting proportions of inhibitory and excitatory mechanisms in the cortex. Indeed, changes in conductance during synaptic activity are determined by the combination of a number of factors: the firing rate of presynaptic neurons, the number of presynaptic neurons, the number of synaptic contacts from each presynaptic neuron, or the conductance change (excitatory or inhibitory) induced at a single contact by a presynaptic action potential, among others. It is estimated that a single pyramidal cell in the cortex receives its input from as many as 1,000 other excitatory neurons (that would make some 5,000 contacts) and as many as 75 inhibitory neurons (that would make some 750 contacts) [31], and the proportion is of 30,000 excitatory against 1,700 inhibitory

for CA1 pyramidal neurons [26]. This anatomical disproportion contrasts with the functional balance between excitation and inhibition. Different factors seem to contribute to the counter-balance of inhibition. Lesser failures of inhibitory transmission achieved by multiple presynaptic contacts from the same inhibitory neuron [40, 45] is one of them, as well as the larger synchronization between inhibitory neurons due to electric coupling [15, 16]. Even more critical is the segregation of inputs onto pyramidal neurons, where inhibitory contacts are restricted to the soma and proximal dendrites [20, 26], while excitatory inputs only innervate further than 50 $\mu$m away from the soma [13, 14]. Not only this results in a larger weight at the soma for inhibitory inputs, but also in a control over the excitatory inputs that reach the soma [2, 36, 48]. There is an additional element and that is the firing rate of inhibitory neurons with respect to excitatory neurons. Fast spiking neurons are known to fire at higher frequencies (Fig. 1b) [25, 28], as a consequence of the presence of $K^+$ channels (Kv3) that allow for a fast repolarization [12] and the lack of fast spike frequency adaptation [10, 25], which can contribute to the excitation/inhibition balance by imposing larger numbers of presynaptic events.

Resolving the contribution of all these mechanisms in achieving the physiological excitation-inhibition balance in the cortex remains a challenge. Current estimations from slow oscillatory activity in the cortex indicate that firing rates differing by around a mere factor of two between regular spiking and fast spiking neurons result in excitatory and inhibitory synaptic conductances that are in balance [17]. This is surprising given the difference in orders of magnitude of the connectivity parameters for excitation and inhibition in the cortex (see above). In order to dissect further the mechanisms that link spiking activity and synaptic current for excitation and inhibition in the cortex, we look here at the relative timing of excitation and inhibition by detecting the times of occurrence of excitatory and inhibitory synaptic events impacting on pyramidal cortical neurons. We then analyze how synaptic event timing and neuronal spiking are related through some connectivity parameters in a computer model of slow oscillatory activity in the cortex [5]. Finally, we discuss the implications that these computational results have in interpreting our experimental findings and their relation to functional structure and dynamics of excitation and inhibition in the cortical network.

## Experimental Procedures and Detection of Synaptic Events

### *Intracellular and Extracellular Recordings In Vitro and In Vivo*

In vitro recordings were obtained as previously described [6, 35] and detailed in the Appendix. In brief, cortical slices from ferret prefrontal or visual cortex were prepared and bathed in an ACSF solution containing ionic concentrations that closely mimic the conditions in situ. In these conditions, spontaneous rhythmic activity (<1 Hz) is generated in the circuit [35]. Recordings were also obtained from

anesthetized rat neocortex (auditory and barrel cortex) [32] and the recorded activity showed the characteristic slow oscillations of this state, which is closely related to slow-wave sleep [41]. Thus, both the in vitro and in vivo preparations reflect a very similar rhythm and are presumably engaging similar mechanisms of the cortical circuit [35].

We investigated the properties of this rhythmic activity in vitro and in vivo by recording intracellularly with sharp electrodes and extracellularly with tungsten electrodes. In all cases, intracellular recordings were recorded in close vicinity of the extracellular recording, in order to relate single-neuron activity to the surrounding population dynamics. For a more detailed methodological description, see the Appendix.

## *Data Analysis*

We used an analysis protocol described elsewhere [6] to identify the timing of excitatory and inhibitory synaptic events recorded intracellularly at different membrane potentials (Fig. 2) and relate them to the ongoing population dynamics (up and down states). The extracellular recording was used to detect the times of transitions between up and down states as illustrated in Fig. 3a and described in the Appendix. From intracellular recordings at different holding voltages, the times of synaptic events were identified as sharp upward or downward deflections in the membrane potential (Fig. 3b, c) and were aligned to the beginning or end of the up state by using the transitions detected from the extracellular recording. This alignment allows to compare the timing of events recorded nonsimultaneously at different holding voltages, because the extracellular recording remains unchanged as the conditions of the intracellular recording are modified. A more detailed description of these methods can be found in the Appendix and in [6].

## *A Short Discussion on the Method*

In order to detect excitatory and inhibitory events in this study we recorded intracellularly from a neuron at membrane potentials that are the reversal potentials of glutamatergic excitation (0 mV) and $GABA_A$ inhibition (−70 mV). In this way, the postsynaptic events that correspond to excitation and inhibition respectively can be isolated. Extremes of the first derivative provide timings for transitions of either EPSPs (if at −70 mV) or IPSPs (if at 0 mV). A threshold is set based on statistical criteria and those events that surpass the threshold separating them from the noise are taken into account as valid synaptic events. An envelope of the local field potential trace determines the times of transition and separates the periods of up and down states. This study focuses on the timing of excitatory and inhibitory events with respect to up and down transitions.

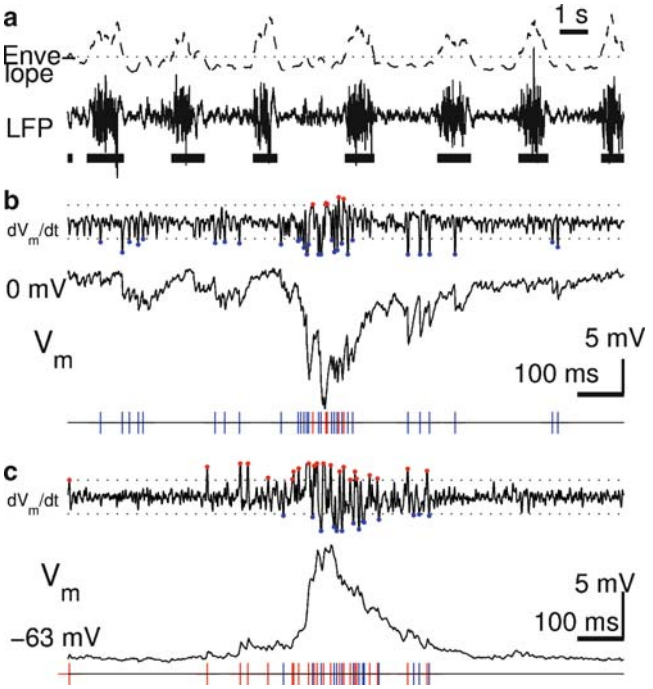


**Fig. 3** Detection of IPSPs and EPSPs during slow oscillations in the cortex. (**a**) Detection of up and down states from the extracellular recording was performed by filtering it between 2 and 150 Hz to obtain a local field potential (LFP) signal. An Envelope was then computed (see the Appendix), from which a simple thresholding allowed us to detect up states (*thick black lines below* LFP). (**b, c**) We detected the timing of synaptic events from each intracellular recording ($V_m$). To this end, we computed its derivative ($dV_m/dt$), and then thresholded it at 2–4 interquartile ranges to detect excitatory events (*red dots*) and inhibitory events (*blue dots*). We did this for an intracellular recording at a depolarized membrane potential (**b**) and at a hyperpolarized membrane potential (**c**) for each neuron, so we could have a more reliable identification of synaptic events of each kind. Because the extracellular recording remained unchanged while we modified $V_m$, aligning event timing to the up state beginning and end (detected from the extracellular record), allowed us to compare the timing of excitatory and inhibitory events. Data shown here correspond to an in vitro recording, but identical methods were applied to in vivo data.

There are some caveats associated to this method. The absolute number of events may be underestimated since those events below threshold are not considered. They may also remain undetected if their rise time is not sharp enough to appear as an independent event, e.g., because they are embedded in a group of events or because they occurred far out in the dendritic arbor. Regarding this, synchronous events may be underestimated by being considered under the same detected event. Because of the higher synchronization of inhibitory neurons [15, 16], this may affect especially inhibitory events. Similarly, slower post-synaptic voltage dynamics will blur post-synaptic responses and induce more false negatives in our detection method. Thus, there may be limitations derived from the different excitatory and inhibitory kinetics

and from the particular distribution of inhibitory connections (soma and proximal dendrites) vs. excitatory connections (distal dendrites). This could bias the detection towards inhibition, since it is going to generate faster events and therefore easier to detect with the first derivative method. Different excitatory and inhibitory potential kinetics could thus bias the detection towards faster, sharper events. Still, the system has been carefully validated in [6], where the influence of threshold on event detection was explored.

Another aspect of this method to consider (and indeed of all conductance detection methods, for a review see [27] is that given that the $V_m$ is held at different values (0, −70 mV) for the detection of IPSPs/EPSPs respectively, the up states that are studied are never the same for both types of events. Still, each quantification of synaptic events (Figs. 5–10) is the result of averaging 17–187 up states, and therefore individual variations between up states are not taken into account. Finally, our derivative method included a low-pass filter with cut-off at 200 Hz. This could also limit the detection of closely spaced events (<5 ms). However, we tested this by repeating the analysis using a cut-off at 500 Hz and we did not find any significant increase in the number of synaptic events detected. Despite all these caveats, this is to our knowledge the only method so far to have an approximation to the timing of the individual synaptic inputs being received by a single pyramidal neuron during physiological network activity. Apart from other possible sources of error, both EPSPs and IPSPs are being recorded ≅70 mV apart from their reversal potential and therefore their driving force should be the same. Our main interest is on the relative timing of both types of events. We consider the method particularly valid on that regard, given that for timing considerations the absolute number of events has been normalized. Still, we dare to have a look into the absolute number of events (see Figs. 5, 8), assuming a comparable error in the detection of excitatory and inhibitory events and considering that we can still learn from their proportions.

## Experimental Results

We applied our synaptic event detection method to $n = 10$ neurons recorded in vitro and $n = 5$ neurons recorded in vivo. For each of these neurons, intracellular recordings of variable duration (range 60–729 s) were obtained, one at a depolarized potential (around 0 mV) and one at a hyperpolarized potential (around −70 mV). A closely adjacent extracellular recording was simultaneously registered to determine the transition times between up states and down states (Fig. 3). We were thus able to obtain putative excitatory events (from the −70 mV recording), and putative inhibitory events (from the 0 mV recording) for each neuron, and attribute them to the up state or down state (as identified from the extracellular signal).

We first extracted general statistics from this analysis, concerning the characteristics of individual EPSPs and IPSPs (Fig. 4, Table 1) and the comparative quantification of synaptic events during up and down states (Table 2). We found that, in vitro, the amplitudes of putative excitatory postynaptic potentials were

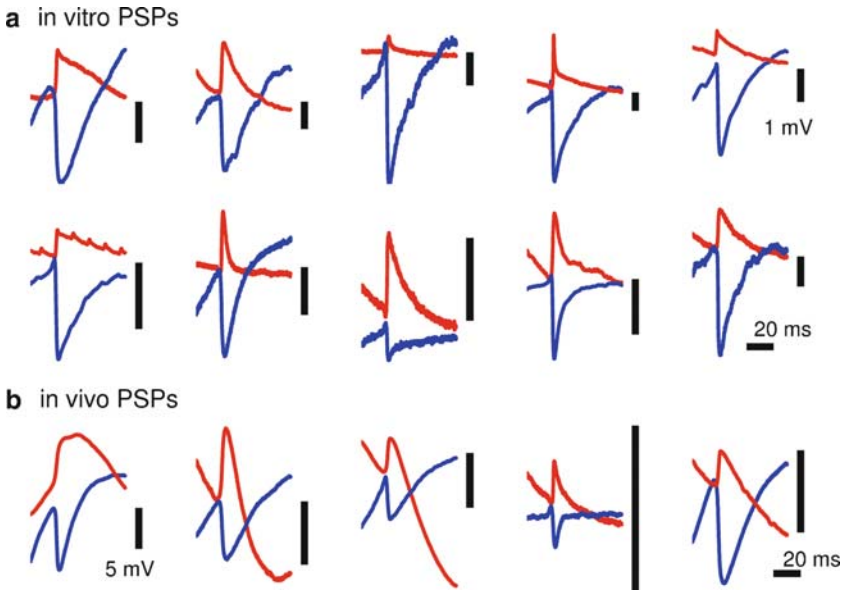


**Fig. 4** Amplitudes and time-course of average post-synaptic potentials for neurons in our database, in vitro (**a**, $n = 10$) and in vivo (**b**, $n = 5$). Inhibitory (excitatory) events were detected from intracellular recordings in neurons held at ∼0 mV (∼−70 mV) as illustrated in Fig. 3. Events that did not occur within 100 ms of other events were used to align pieces of the intracellular signal and average them to obtain the average inhibitory (*blue*) and excitatory (*red*) post-synaptic potentials. Different number of events were used for averaging each trace, ranging from 17 to 187 in vitro, and 70 to 846 in vivo. Each panel shows averages for a given neuron in our database. Vertical calibration bars indicate 1 mV in (**a**) and 5 mV in (**b**). The time base is the same for all panels, as indicated in the last set of traces in each panel.

**Table 1** Amplitude and decay time of $V_m$ deflections for isolated synaptic events (no other event occurring in a 100-ms window) detected at either depolarized ($V_m \sim 0$ mV) or hyperpolarized ($V_m \sim -70$ mV) voltages (Fig. 4)

| | In vitro recordings ($n = 10$) | | | In vivo recordings ($n = 5$) | |
|---|---|---|---|---|---|
| | $V_m \sim 0$ mV | | $V_m \sim -70$ mV | $V_m \sim 0$ mV | $V_m \sim -70$ mV |
| Amplitude of isolated events | 2.58 ± 0.45 mV (0.44–5.23 mV) | > | 1.17 ± 0.21 mV (0.41–2.67 mV) | 4.6 ± 1.1 mV (1.2–7.4 mV) | 3.6 ± 0.96 mV (1.2–6.3 mV) |
| Decay time of isolated events | 27.9 ± 10.1 ms (0.66–13.8 s) | | 28 ± 13 ms (3–127 ms) | 31 ± 10 ms (4–52 ms) | 33 ± 13 ms (7–62 ms) |

Population data is reported as mean ± s.e.m. and ranges are indicated in parenthesis. Significant differences (paired $t$-test, $p < 0.05$) are indicated with the symbol>

significantly smaller than those of putative inhibitory postsynaptic potentials (paired $t$-test, $p = 0.007$). Such difference was not detected in vivo (Table 1). We did not detect differences in the decay dynamics of synaptic events either in vivo or in vitro. Regarding up and down states (Table 2), we found that up states were significantly

**Table 2** Comparative statistics of excitatory and inhibitory events during up and down states in vitro and in vivo

| | In vitro recordings ($n = 10$) | | | In vivo recordings ($n = 5$) | | |
|---|---|---|---|---|---|---|
| | Up states | | Down states | Up states | | Down states |
| Duration | $878 \pm 66$ ms$^{\dagger}$ (531–1,607 ms) | $<$ | $3.21 \pm 0.77$ s (0.66–13.8 s) | $792 \pm 296$ ms$^{\dagger}$ (342–2,172 ms) | | $580 \pm 86$ ms$^{\dagger}$ (329–886 ms) |
| No. detected excitatory events | $27 \pm 5$ (14–65) | | $15.7 \pm 8.9$ (0–19) | $25.9 \pm 12.2$ (4–72) | | $16.1 \pm 6.4$ (1–36) |
| No. detected inhibitory events | $24 \pm 4$ (13–53) | | $18.5 \pm 9.3$ (0–81) | $19.3 \pm 5.5$ (10–39) | | $10.4 \pm 4.3$ (1–26) |
| Rate detected excitatory events | $36.6 \pm 5.8$ s$^{-1\ddagger}$ (10–73 s$^{-1}$) | $>$ | $3.2 \pm 0.8$ s$^{-1}$ (0.2–7.2 s$^{-1}$) | $33.5 \pm 10$ s$^{-1\ddagger}$ (7–67 s$^{-1}$) | $>$ | $25.2 \pm 8.9$ s$^{-1\ddagger}$ (1.5–56 s$^{-1}$) |
| Rate detected inhibitory events | $26.7 \pm 2.5$ s$^{-1\ddagger}$ (15–43 s$^{-1}$) | $>$ | $5.9 \pm 2.1$ s$^{-1}$ (0.1–23 s$^{-1}$) | $31.4 \pm 7.7$ s$^{-1\ddagger}$ (16–60 s$^{-1}$) | $>$ | $21.1 \pm 9.5$ s$^{-1\ddagger}$ (2–57 s$^{-1}$) |

Population data is reported as mean $\pm$ s.e.m. and ranges are indicated in parenthesis. Significant differences (one-tailed paired $t$-test, $p < 0.05$) are indicated with the symbols $>$ and $<$. † This is an over-estimate, as states shorter than 250 ms were discarded from the analysis. ‡ This is an under-estimate, because of the over-estimation in †

shorter than down states in vitro (one-tailed paired $t$-test, $p = 0.0037$, $n = 20$), but not so in vivo (paired $t$-test $p = 0.2$, $n = 5$). Synaptic event rates were always significantly higher in the up states than in the down states, both in vitro and in vivo, although the difference was more accentuated in vitro.

Comparing the statistics numbers between in vivo and in vitro, we found that up state durations were comparable between the two conditions (two-sample $t$-test, $p = 0.64$), but down state durations were significantly shorter in vivo than in vitro (two-sample $t$-test, $p = 0.023$). The amplitudes of excitatory postsynaptic events were significantly smaller in vitro than in vivo (two-sample $t$-test, $p = 0.006$), but their kinetics were comparable. Regarding detected synaptic events, only the rate of events during the down state differed significantly between these two conditions (two-sample $t$-test, $p < 0.05$). Inhibitory events occurred significantly more frequently in the down state in vivo than in vitro ($p = 0.004$), and excitatory events showed a similar, marginally significant trend ($p = 0.054$). This result indicates the presence of more basal synaptic activity in vivo than in vitro, and also shows that network activations in the two conditions do not differ significantly.

## *Excitatory and Inhibitory Events During Risetime of Up States In Vitro*

For each neuron, excitatory and inhibitory events detected intracellularly were aligned at the time of up state initiation, as detected in the neighboring simultaneous extracellular recording (Fig. 3). Synaptic event histograms (in bins of 5 ms) were then averaged across neurons after realigning them to the steepest increase in excitatory synaptic events (arbitrarily considered time zero, see Fig. 7). In terms of detected event rate, we found no consistent difference between the event rate of

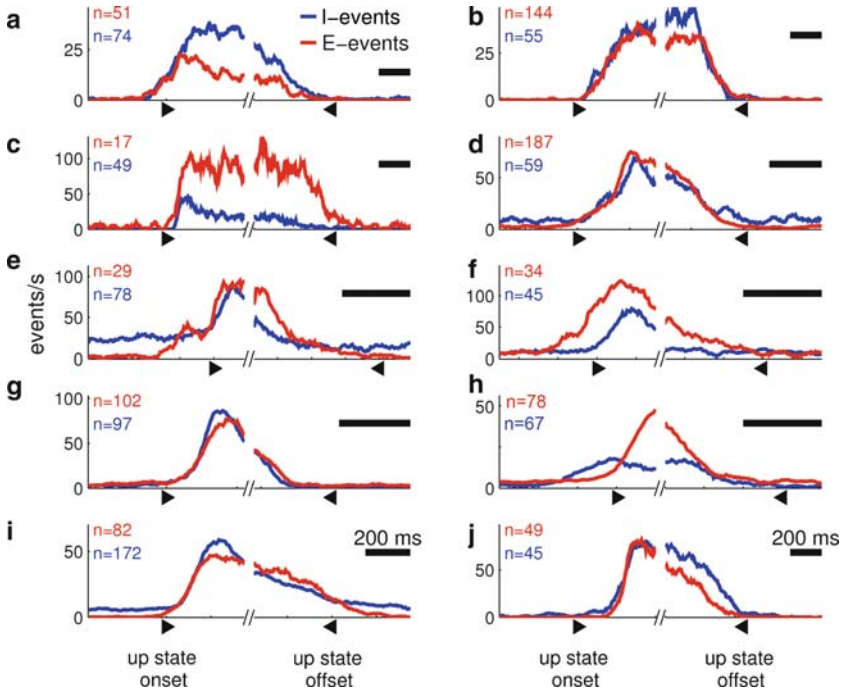


**Fig. 5** Synaptic event rates through the duration of the up state in each of 10 neurons in vitro. Time-histograms of synaptic events detected from intracellular records (Fig. 3) and aligned to up state onset (►) or up state offset (◄), as detected from the extracellular record (Fig. 3). Excitatory events (*red*) arrive at a higher peak rate than inhibitory events (*blue*) in (**c**), (**f**) and (**h**), whereas the opposite is true in (**a**). For the rest of panels, peak event rate is approximately similar for excitatory and inhibitory events. For each trace, the number $n$ of up states from which spike events were gathered is indicated. Horizontal calibration bars indicate 200 ms.

excitation and inhibition during the up state in vitro (Fig. 5). While some neurons showed a higher peak rate of excitatory events (Fig. 5c, f, h), others showed a higher peak rate for inhibitory events (Fig. 5a), and most ($n = 6/10$) presented approximately equal rates for both types of events. Such a delicate balance of event rate between excitation and inhibition is remarkable. Even when the method used may have a number of limitations (see above), it seems unlikely that this almost identical number could be reached by chance. When the normalized risetime of EPSPs/IPSPs to their maximal event rate was evaluated, individual neurons showed in most cases ($n = 8/10$) a matching time course for excitation and inhibition (Fig. 6). From the other two cells, one shows an early rise of excitation (by ∼50 ms, Fig. 6f) and the other one of inhibition (by ∼20 ms, Fig. 6h). The occurrence of excitatory and inhibitory events during the risetime of up states averaged across cells revealed that the increase in both types of events is synchronous in our population of in vitro

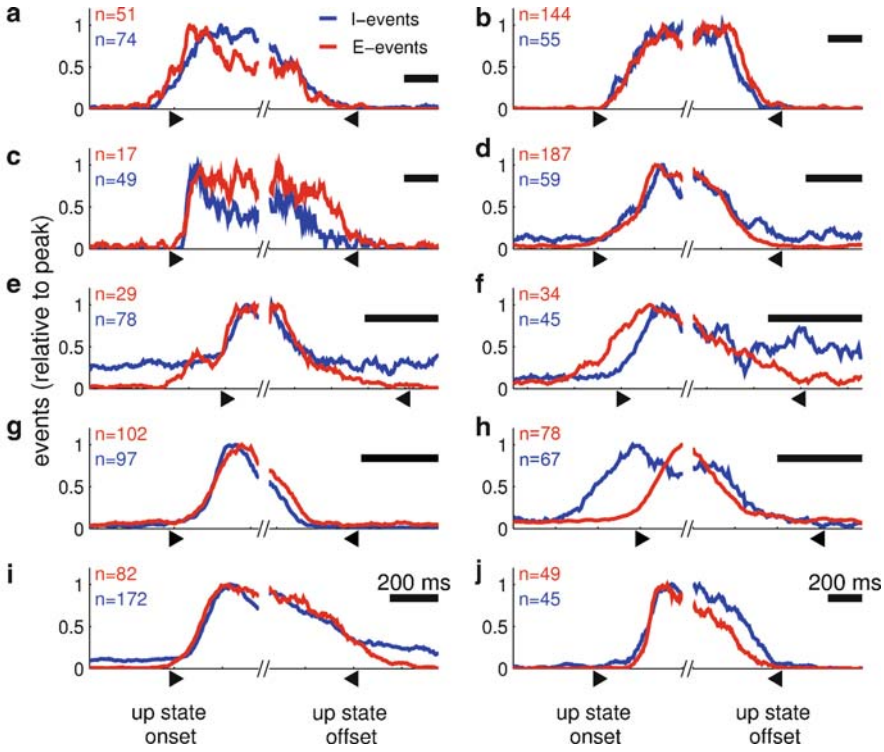


**Fig. 6** Normalized synaptic events through the duration of the up state in each of 10 neurons in vitro. Time-histograms of synaptic events from Fig. 6 were normalized to peak event rate to compare the dynamics of excitation and inhibition at up state onset (►) and at up state offset (◄). During up state onset, excitatory events (*red*) increase ahead than inhibitory events (*blue*) in (**f**), whereas the opposite is true in (**h**). For the rest of panels, excitatory and inhibitory events increase to their maximal rate at approximately the same point in time. Also extinction at up state offset occurs concomitantly for excitation and inhibition, except in (**b**), (**c**), and (**g**) (excitation outlasts inhibition) and in (**h**) and (**j**) (inhibition outlasts excitation). For each trace, the number *n* of up states from which spike events were gathered is indicated. Horizontal calibration bars indicate 200 ms.

recordings. The take off from the down state occurs simultaneously, with no significant deviation between excitation and inhibition until well after the peak in PSPs is reached (Fig. 7a, b).

## *Excitatory and Inhibitory Events During the End of Up States In Vitro*

In order to analyze the occurrence of excitatory and inhibitory events during the termination of the up states, synaptic events in each cell were aligned at the offset of the up state, as detected from extracellular recordings, and then realigned to

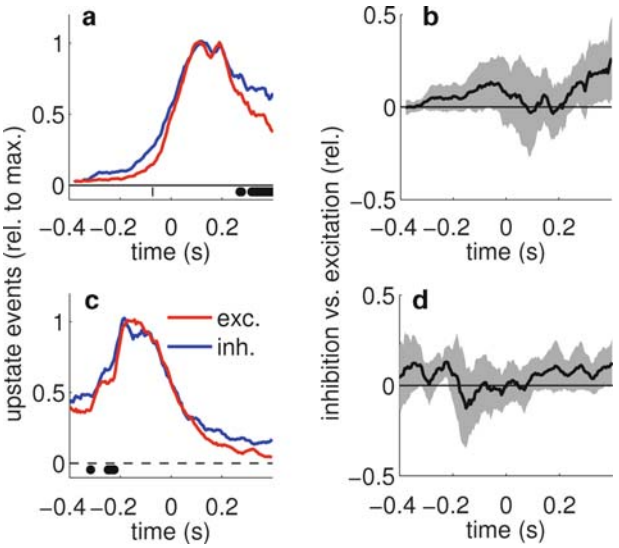


**Fig. 7** Population analysis of EPSPs/ IPSPs timing at the beginning and end of the up states in vitro. (**a**) Excitatory (*red*) and inhibitory (*blue*) synaptic events detected from intracellular recordings in vitro ($n = 10$) accumulated at comparable rate at the onset of the up state. Synaptic event histograms from Fig. 7 were averaged across neurons after aligning them to the steepest increase in excitatory synaptic events (corresponding to time zero in **a**, **b**). (**b**) Difference in event accumulation to peak event rate between inhibition and excitation (*black line*). Positive (negative) values indicate excess of inhibition (excitation). *Gray shadow* is the 95% confidence interval calculated with a jackknife procedure over neurons ($n = 10$). During up state onset, there was no significant difference in the time of fastest accumulation of excitatory and inhibitory events. Periods with significant difference between excitation and inhibition are marked on **a** with a thick black line along the *x*-axis. (**c**) Same as **a**, but synaptic events into each cell were aligned at the offset of the up state (◄ in Fig. 6), and then realigned to the steepest decrease in the excitatory histogram before computing the average over neurons. (**d**) Same as **b** for the data in **c**. Synaptic event extinction at the end of the up state did not differ for excitation and inhibition at the 95% confidence level.

the steepest decrease in the excitatory histogram before computing the average over neurons (Fig. 7c, d). When the average obtained in this way is observed, we can see that the peak in both EPSPs and IPSPs before the transition to the down state is initiated is reached at the same time. From that moment, the decrease in excitation and inhibition is in average mostly synchronous, with no significant difference between both within a 95% confidence interval (Fig. 7c, d). When we look at individual neurons, the relation between excitation and inhibition during up state termination is more heterogeneous than during its initiation (Fig. 6). While in 5 out of 10 neurons, there is a synchronous decrease in EPSPs and IPSPs, in 4 out of 10 the decrease in inhibition precedes that of excitation in time, although with a similar time course (Fig. 6b, c, g, h). In just one case, it is the excitation the one that decreases first, followed by inhibition (Fig. 6j). Therefore, even when the result of the average suggests an equilibrium between the timing of decrease of EPSPs and IPSPs at the

end of the up states, the EPSPs and IPSPs at the end of the up states, the individual cases heterogeneity also exists regarding the absolute number of excitatory and inhibitory events. Even when the general trend gravitates towards the comparable number in both cases, individual neurons display either larger numbers of EPSPs or IPSPs (Fig. 5).

In spite of individual variations, we conclude that when the timing of excitatory and inhibitory events is analyzed during the risetime and the repolarization of the up states in vitro it is noteworthy that both events increase to start an up state, and decrease to finish it up with a remarkable synchrony. Furthermore, the total number of events, even within certain individual variability, could be considered to be quite similar, in at least half the neurons virtually identical.

## *Excitatory and Inhibitory Events During Risetime of Up States In Vivo*

For each neuron, events detected intracellularly were aligned at the time of up state initiation, as detected in the neighboring simultaneous extracellular recording. Synaptic event histograms were then averaged across neurons after realigning them to the steepest increase in excitatory synaptic events (corresponding to time zero in Fig. 10a, b). During up state onset, there was no significant difference between excitation and inhibition rate of increase in our population of in vivo recordings (Fig. 10a, b, $n = 5$), quite similarly to what was observed in vitro (Fig. 7). Different from in vitro was, though, a faster rate in the accumulation of synaptic events. Excitatory events accumulated at a rate of 1.307%/ms (range 0.309–3.93%/ms) in vitro and 1.815%/ms (range 0.312–4.97%/ms) in vivo. Inhibitory events accumulated at a rate of 1.380%/ms (range 0.533–3.32%/ms) in vitro and 1.704%/ms (range 1.396–2.076%/ms) in vivo. Although nonsignificant (two-sample $t$-test $p > 0.5$; Wilcoxon rank sum test $p > 0.3$, $n = 10, 5$), the trend in difference between in vitro and in vivo measurements agrees with what is observed at the membrane level (Figs. 1 and 2), where transitions between up and down states are often faster in vivo than in vitro.

Another interesting difference between in vitro and in vivo conditions revealed by the average of synaptic events is the decay in accumulated EPSPs as soon as the up state is reached (Fig. 10a), what could be the result of spike frequency adaptation in pyramidal neurons, and/or synaptic depression in excitatory synapses to pyramidals. This time course observed for excitatory events is not followed by inhibitory events, that remained in a plateau once the up state was reached. Note that this analysis is normalized and provides information about timing of occurrence, but not about the absolute number of excitatory/inhibitory events.

Focusing on individual neurons, the normalized events (Fig. 9) are indicative of a remarkable analogous timing of accumulation of excitatory and inhibitory events in vivo as well as in vitro (see above). Even when there is a slight variation in 2 out of 5 cases, the predominant trend is a well synchronized accumulation of events. If the

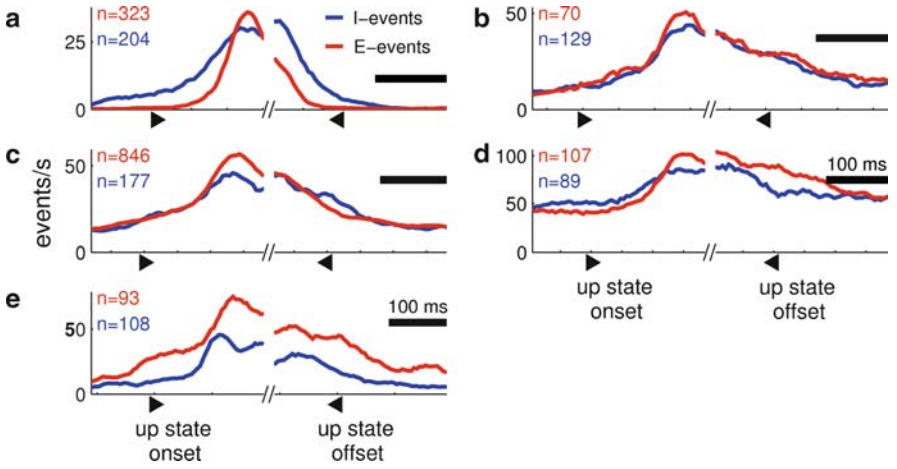


**Fig. 8** Synaptic event rates through the duration of the up state in each of 5 neurons in vivo. Time-histograms of synaptic events detected from intracellular records (Fig. 3) and aligned to up state onset (►) or up state offset (◄), as detected from the extracellular record (Fig. 3). Excitatory events (*red*) arrive at a higher peak rate than inhibitory events (*blue*) in all panels, but only in (**e**) the difference was sizeable. For each trace, the number *n* of up states from which spike events were gathered is indicated. *Horizontal calibration bars* indicate 100 ms.

absolute – and not the normalized – number of events is considered, the same trend is maintained, although it allows to evaluate the relative number of events (Fig. 7). In all five neurons studied here the absolute number of excitatory synaptic events that lead to the up state is larger than that of inhibitory events, but for a proportion not larger than 25% (except in Fig. 8e, where the excess of excitatory events is around 50%).

## *Excitatory and Inhibitory Events During the End of Up States In Vivo*

Synaptic events in each cell were aligned at the offset of the up state, as detected from extracellular recordings, and then realigned to the steepest decrease in the excitatory histogram before computing the average over neurons (Fig. 10c, d). The average across five neurons recorded in vivo revealed a simultaneous decay in the rate of occurrence of EPSPs and IPSPs, although for a brief time (few tens of ms) excitatory events extinguished earlier than inhibitory ones, as assessed at the 95% confidence level (Fig. 10c, d). A larger sample would be necessary to confirm this trend.

The timing of synaptic events at the end of the up states for individual neurons is illustrated in Fig. 9. Again, the simultaneous decrease of both excitatory and inhibitory events is striking in these plots. When each individual case is explored in detail, we can see that both excitatory or inhibitory events can lead the extinction

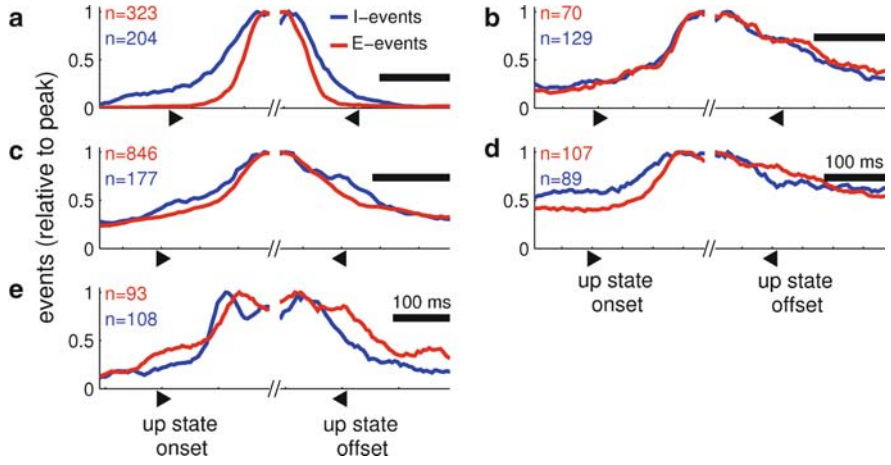


**Fig. 9** Normalized synaptic events through the duration of the up state in each of 5 neurons in vivo. Time-histograms of synaptic events from Fig. 9 were normalized to peak event rate to compare the dynamics of excitation and inhibition at up state onset (►) and at up state offset (◄). During up state onset, inhibitory events (*blue*) increase ahead than excitatory events (*red*) in (**a**), (**c**), and (**d**). For the rest of panels, excitatory and inhibitory events increase to their maximal rate at approximately the same point in time. Extinction at up state offset occurs first for excitation in (**a**) and (**c**), first for inhibition in (**e**), and concomitantly for excitation and inhibition in (**b**) and (**d**). For each trace, the number *n* of up states from which spike events were gathered is indicated. Horizontal calibration bars indicate 100 ms.

of synaptic events, but that the time course of the decay is invariably similar. If the absolute number of events are evaluated (Fig. 8), then it can be observed that the similarity of time course can indeed conceal a remarkable difference in the number of synaptic events.

## Excitation and Inhibition in Up and Down states Generated in a Cortical Model

The results of our experimental study of excitation and inhibition are difficult to reconcile with the predictions of the computer model of slow oscillatory activity ([5]; Fig. 11a). This computer model can reproduce intracellular and extracellular data of slow oscillatory activity in cortical slices [35], with interneurons and pyramidal neurons firing practically in phase through the slow oscillation (Fig. 11b). Excitatory and inhibitory conductances were found to maintain a proportionality in this model, as found experimentally [38]. Model inhibitory neurons display a higher firing rate during up states (ca. 30 Hz) while excitatory neurons have a firing frequency which is lower (ca. 15 Hz) (for comparison with experimental results see Fig. 1). However, one feature of the model seems at odds with the experimental results reported here. The presynaptic firing of model inhibitory neurons leads the beginning of the

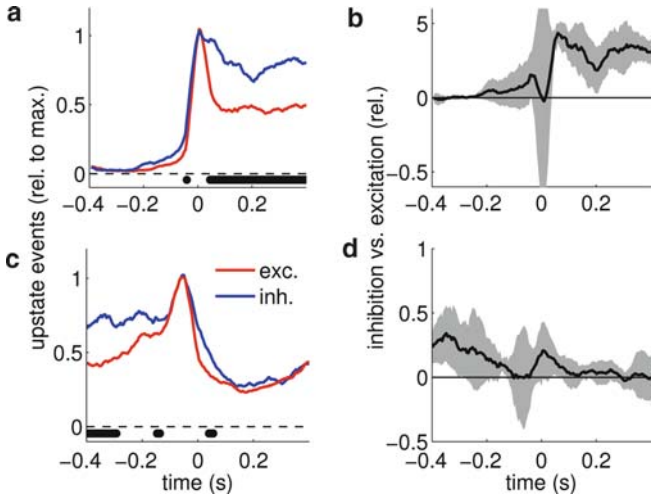


**Fig. 10** Population analysis of EPSPs/IPSPs timing during the beginning and end of the up states in vivo. (**a**) Excitatory (*red*) and inhibitory (*blue*) synaptic events detected from intracellular recordings in vivo ($n = 5$) accumulated at comparable rate at the onset of the up state. Normalized synaptic event histograms (Fig. 10) were averaged across neurons after aligning them to the steepest increase in excitatory synaptic events (corresponding to time zero in **a**). (**b**) Difference in event accumulation to peak event rate between inhibition and excitation (*black line*). Positive (negative) values indicate excess of inhibition (excitation). Gray shadow is the 95% confidence interval calculated with a jackknife procedure over neurons ($n = 5$). During up state onset, there was no significant difference between excitation and inhibition rate of increase. However, a significant fraction of excitatory events remained confined to a short time window after up state initiation, possibly indicating adaptation dynamics. Instead, inhibitory events remained constant over up state duration. (**c**) Same as (**a**), but synaptic events into each cell were aligned at the offset of the up state, and then realigned to the steepest decrease in the excitatory histogram before computing the average over neurons. (**d**) Same as **b** for the data in **c**. Inhibitory synaptic events extinguished later than excitatory synaptic events during the transition from the up state to the down state, as assessed at the 95% confidence level.

up states by tens of milliseconds and persists at their ending (Fig. 11c). In contrast, in our experiments we found that synaptic events detected intracellularly, both in vitro and in vivo, showed a remarkable matching of both event rate and timing of onset for excitatory and inhibitory events. We therefore turned back to our computer model to explore mechanistically the compatibility between the model and the experimental results regarding the timing and event rate magnitude of excitation and inhibition during the slow oscillation.

## *Modeling the Cortex*

We used the network model of [5], with exactly the same parameters as in their control condition. Briefly, the network model consists of a population of 1024 pyramidal

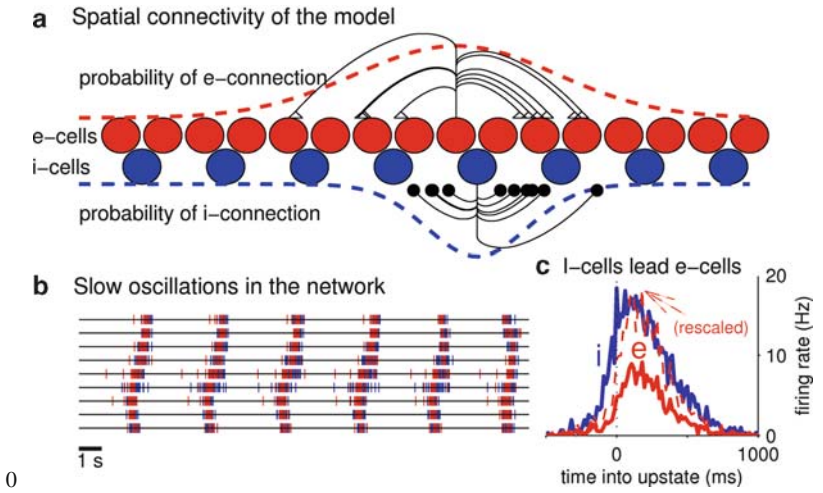


**Fig. 11** Model architecture and function: i-cells lead e-cells during up state initiation. (**a**) The model consisted of excitatory (*red*) and inhibitory (*blue*) neurons (in a relation 4:1) connected through conductance-based synapses. The existence of a functional synapse between any two neurons was decided at the beginning of the simulation based on a Gaussian probability distribution. The footprint $\sigma$ of this connectivity distribution could differ for excitatory and inhibitory connections. In the control case in [5], $\sigma_E = 2\sigma_I$. Each neuron only had a limited number of postsynaptic partners. In the control network in [5], both pyramidals and interneurons connected to 20 pyramidal neurons and 20 interneurons, respectively. (**b**) Sample network activity, shown as an array of multiunit spike trains, reflects slow oscillatory activity with interneurons (*blue*) and pyramidal neurons (*red*) firing in phase during the slow oscillation. (**c**) A closer look at neuronal activity around the time of up state initiation, shows that interneurons rise to their maximal firing rate ahead of closely adjacent pyramidal neurons (Adapted with permission from Figs. 2 and 3 in [5].).

cells and 256 interneurons equidistantly distributed on a line and interconnected through biologically plausible synaptic dynamics (Fig. 11a). Some of the intrinsic parameters of the cells are randomly distributed, so that the populations are heterogeneous. This and the random connectivity are the only sources of noise in the network.

Our model pyramidal cells have a somatic and a dendritic compartment. The spiking currents, $I_{Na}$ and $I_K$, are located in the soma, together with a leak current $I_L$, a fast A-type $K^+$-current $I_A$, a noninactivating slow $K^+$-current $I_{KS}$ and a $Na^+$-dependent $K^+$-current $I_{KNa}$. The dendrite contains a high threshold $Ca^{2+}$ current $I_{Ca}$, a $Ca^{2+}$-dependent $K^+$-current $I_{KCa}$, a noninactivating (persistent) $Na^+$ current $I_{NaP}$ and an inward rectifier (activated by hyperpolarization) noninactivating $K^+$ current $I_{AR}$. Explicit equations and parameters for these Hodgkin–Huxley-type currents can be found in [5]. In our simulations, all excitatory synapses target the dendritic compartment and all inhibitory synapses are localized on the somatic compartment of postsynaptic pyramidal neurons. Interneurons are modeled with just Hodgkin–Huxley spiking currents, $I_{Na}$ and $I_K$, and a leak current $I_L$ in their single compartment [50]. Model pyramidal neurons set according to these parameters fire

at an average of 22 Hz when they are injected a depolarizing current of 0.25 nA for 0.5 s. The firing pattern corresponds to a regular spiking neuron with some adaptation. In contrast, a model interneuron fires at about 75 Hz when equally stimulated and has the firing pattern of a fast spiking neuron.

Synaptic currents are conductance-based and their kinetics are modeled to mimic AMPAR-, NMDAR-, and $GABA_A$ R-mediated synaptic transmission [5,49]. All parameters for synaptic transmission are taken from the control network in [5]. These values were chosen so that the network would show stable periodic propagating discharges with characteristics compatible with experimental observations.

The neurons in the network are sparsely connected to each other through a fixed number of connections that are set at the beginning of the simulation. In our control network, neurons make $20 \pm 5$ contacts (mean $\pm$ standard deviation) to their postsynaptic partners (multiple contacts onto the same target, but no autapses, are allowed). For each pair of neurons, the probability that they are connected in each direction is decided by a Gaussian probability distribution centered at 0 and with a prescribed standard deviation.

The model was implemented in C++ and simulated using a fourth-order Runge–Kutta method with a time-step of 0.06 ms.

## *Excitatory and Inhibitory Events During Up States In Computo*

We analyzed spiking activity in inhibitory and excitatory neurons, and the timing of excitatory and inhibitory synaptic events into excitatory neurons, averaging data from five different network simulations (with different noise realizations to define the connectivity and neuron properties). We confirmed that the average firing rates of neurons followed the results reported in [5], namely that inhibitory neurons fired at higher rates (Fig. 12b), and increased earlier to their maximal rate (Fig. 13b) than excitatory neurons in our control network model. However, when the rates of incoming synaptic events into excitatory neurons were analyzed we found that the peak rate of excitatory events exceeded that of inhibitory events (Fig. 12a), while both excitatory and inhibitory events raised to their maximal rate in synchrony (Fig. 13a). These results may appear paradoxical: although interneurons fired more and ahead in time, inhibitory event rate was lower and did not show appreciable advance with respect to excitatory event rate. This reflects the multiple parameters that link firing rate to incoming synaptic rates, to the point of being able to distort significantly the relative values for excitation and inhibition, both in magnitude and timing. We examined this point in the model by testing two specific parameters that define the connectivity in our model network.

The relative length of excitatory and inhibitory horizontal connections in our network controlled the relative timing of arrival of excitatory and inhibitory events into model neurons. In the control network, excitatory neurons connected to other neurons in the network with a symmetric Gaussian probability distribution of standard deviation $\sigma_E$ twice as large as the standard deviation $\sigma_I$ of inhibitory projections

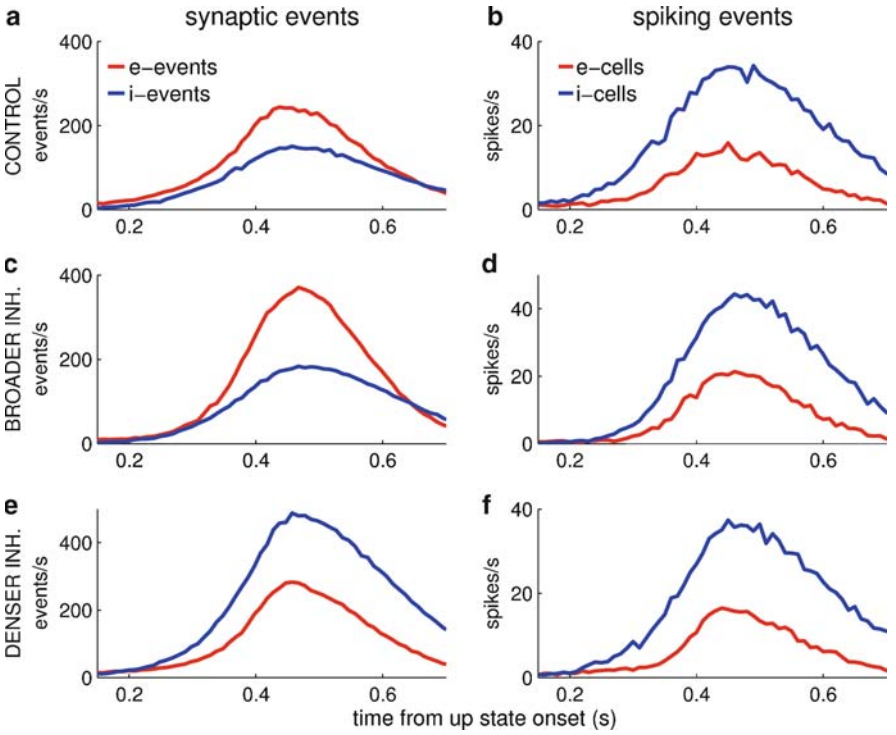


**Fig. 12** Rate of excitatory and inhibitory synaptic events and spiking of excitatory and inhibitory neurons during the beginning and end of the up states in computo. (**a**) Rate of synaptic events (*red* = excitatory, *blue* = inhibitory) into pyramidal neurons and (**b**) Firing rate of adjacent excitatory (*red*) and inhibitory (*blue*) neurons during the up state in the computational network model of slow oscillatory activity [5]. In the model, although inhibitory neurons fire at more than double the rate than excitatory neurons, the rate of synaptic events coming into an excitatory neuron is higher for excitation than inhibition. This is due to the larger fraction of excitatory neurons in the network and their approximately equal connectivity (all neurons have 20 postsynaptic partners of each kind, excitatory or inhibitory). One-minute-long simulation data from 128 neurons equidistantly spaced along the network were used for the analysis. When the divergence of inhibitory connections was increased (by a factor four), firing rates increased slightly (**d**) and so did synaptic event rates (**c**). When inhibition was made denser than excitation by increasing twofold the number of synaptic contacts that each interneuron makes, inhibitory synaptic event rates increased markedly (**e**) whereas firing rates remained unaffected (**f**).

(Fig. 11a). Excitatory neurons had longer horizontal connections than inhibitory ones. Thus, when a front of activity propagated along the network, changes in excitatory rates were projected to neurons further away than changes in inhibitory rates. This compensated for the delayed firing of excitatory neurons at up state onset (Fig. 13b), and neurons received synchronous increases of excitatory and inhibitory synaptic events (Fig. 13a). These synaptic events caused firing first in the inhibitory neurons, possibly because of their lower firing threshold and their faster time constant. To test this mechanistic interpretation, we modified the relative footprint of

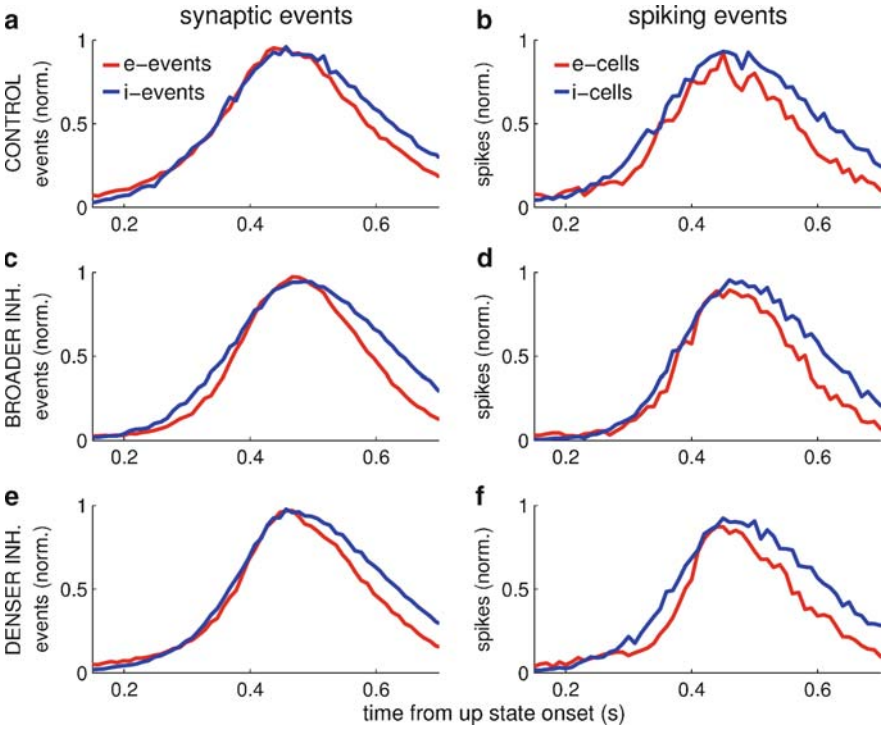


**Fig. 13** Timing of excitatory and inhibitory synaptic events and spiking of excitatory and inhibitory neurons during the beginning and end of the up states in computo. (**a**) Rate of synaptic events normalized to peak event rate (*red* = excitatory, *blue* = inhibitory) into pyramidal neurons and (**b**) Normalized firing rate of adjacent excitatory (*red*) and inhibitory (*blue*) neurons during the up state in the computational network model of slow oscillatory activity [5]. In the model, although inhibitory neurons increase to their maximal rate ahead than excitatory neurons during up state onset (**b**), the accumulation of synaptic events coming into an excitatory neuron is equal for excitation than inhibition (**a**). This is due to the broader connectivity footprint for excitation than for inhibition. When the divergence of inhibitory connections was increased (by a factor four), inhibitory rates still accumulated slightly ahead than pyramidal neurons (**d**) and so did now synaptic event rates, too (**c**). When inhibition was made denser than excitation by increasing twofold the number of synaptic contacts that each interneuron makes, the timing relations of the control network (**a**, **b**) were not affected: synaptic event rates varied concomitantly for excitation and inhibition (**e**) and interneurons increased their firing ahead than pyramidals (**f**). In all cases, inhibitory events (neurons) outlasted excitatory events (neurons) at the end of the up state.

excitatory and inhibitory connections to make inhibitory projections more divergent ($\sigma_I = 2\sigma_E$). We found that the slight advance in inhibitory neuron firing rate increase at up state onset (Fig. 13d) was mimicked by an advanced arrival of inhibitory events to excitatory neurons in the network (Fig. 13c). In this case, because excitatory projections did not exceed the inhibitory footprint, they could not compensate interneuron advanced firing at up state onset. This manipulation also

increased slightly the event rates and firing rates of neurons during the self-sustained slow oscillation, but did not modify the relative magnitudes between excitation and inhibition (Fig. 12c, d).

The average number of connections that each cell type made with postsynaptic neurons of either kind in the network were parameters that controlled the relative magnitude of inhibitory and excitatory synaptic event rates. In the control network, although inhibitory neurons fired at a higher rate (Fig. 12b), because there were four times more excitatory neurons in the network, and excitatory and inhibitory neurons made the same average number of contacts on postsynaptic neurons, the rate of excitatory events received by postsynaptic neurons exceeded by a significant factor the rate of inhibitory events (Fig. 12a). Instead, if we manipulated the connectivity of the network and had interneurons make more postsynaptic contacts on average than excitatory neurons (per i-cell, 80 $\pm$ 5 inhibitory contacts to e-cells, same to i-cells; per e-cell, 20 $\pm$ 5 excitatory contacts to e-cells, same to i-cells; mean $\pm$ s.d. Concomitantly to this increase in number of inhibitory synapses, we diminished the conductance of an individual inhibitory synapse by a factor $^1/_4$, so that overall inhibitory currents remained unchanged), we found that the number of inhibitory events received by pyramidal neurons now exceeded that of excitatory events (Fig. 12e) by approximately the same ratio as in neuronal firing rates (Fig. 12f). This is consistent with the fact that the neuronal ratio of 4:1 in cell number (excitatory to inhibitory) was now compensated by a connectivity contact ratio of 1:4, so spiking events translated by a common factor to synaptic events and maintained their relative relationship. Notice that neuronal firing rates during the up states of the slow oscillations did not change appreciably with respect to the control network (Fig. 12f compared with Fig. 12b), because of the rescaling of inhibitory conductances to compensate the increase in inhibitory connectivity. In relation to the timing of excitation and inhibition at up state onset, this manipulation did not induce any appreciable change relative to the control case (Fig. 13a, b): Interneurons kept firing ahead than pyramidal neurons at up state onset (Fig. 13f), but inhibitory and excitatory events arrived in synchrony to their postsynaptic targets (Fig. 13e).

We found that in our model network, inhibitory firing and inhibitory synaptic events outlasted in all cases excitation at the end of the up state (Fig. 13). This persistence of inhibitory events after excitatory event extinction was accentuated when the footprint of inhibitory projections was increased (Fig. 13c), as would be expected. This effect was seen in some of the experimental recordings (Fig. 6h, j and Fig. 9a), but was not generally true in our population of neurons in vitro (Fig. 7c), although it appeared significant in our small sample of in vivo neurons (Fig. 10c).

## Timing of Excitation and Inhibition in Cortical Activity

Here we have analyzed the timing of inhibitory and excitatory events during the up and down states occurring in the cortex in vitro, in vivo, and in a computer model.

An equilibrium between excitation and inhibition in the recurrent network of the cerebral cortex has been proposed to be critical to maintain the stability of its

function. Changes in excitatory and inhibitory conductances in vitro reveal that both increase and decrease at the beginning/end of up states in close association with each other [38]. Not only in time, but also the amplitude of both were related, with a slope of 0.68 ($G_i/G_e$) in the aforementioned study. Our approach is different, and provides information regarding timing of both types of events as well as an estimation of the number of events. In agreement to what was reported in [38], we find a remarkable coincidence in the accumulation of both excitatory and inhibitory events during the rise of an up state, suggesting reverberation of activity in the local cortical microcircuits. In six out of ten cases the absolute number of excitatory and inhibitory synaptic events recorded from neurons in vitro is very similar as well.

Individual pyramidal neurons receive on average inputs from 1,000 excitatory neurons vs. 75 inhibitory ones, resulting in a number of contacts of 5,000 vs. 750, respectively [31]. Besides, most of cortical neurons participate in up states [41]. The open question is then, how can the number of excitatory and inhibitory events received by a pyramidal neuron be similar? A simple answer to it is the higher firing rate of inhibitory neurons, that would compensate for the lesser number of inhibitory synaptic connections. Cortical fast spiking neurons, known to be gabaergic [19,45], have steeper input–output (intensity-frequency) relationships [25, 28] as a result of their intrinsic properties [12]. Furthermore, fast spiking neurons respond with much longer trains of action potentials when activated synaptically during up states [38]. We and others [43] have also observed that the firing of fast spiking neurons activated synaptically during up states [38]. We and (Fig. 1) although we have not carried out a systematic fast spiking neurons during up states is higher than that of rate could compensate, at least in part, for the lesser number of inhibitory presynaptic contacts. In spite of the disproportion between anatomical excitatory and inhibitory contacts onto pyramidal cells, not only did we find that there are similar numbers of excitatory and inhibitory events but also that the inhibitory ones are of significantly larger average amplitude (2.78 mV) than the excitatory ones (0.8 mV) in vitro. Somatic and proximal innervation of gabaergic inputs is probably a main factor on this difference, although synchrony of inputs due to presynaptic electrical coupling could also contribute [15, 16]. Even when we consider that the caveats of this method (see section “A Short Discussion on the Method”) would equally affect both IPSPs and EPSPs, the possibility remains that one of them was consistently underestimated. The method used here could result in an overestimation of inhibitory synaptic events with respect to the excitatory ones. Inhibition occurs in the soma or proximal dendrites [13, 14] while excitation takes place further away from the soma. Therefore, excitatory events would have smaller amplitudes and remain below threshold, or because occurring further away from the soma, their kinetics are slower and they are more difficult to detect. We cannot rule out that possiblity. However, our detection procedure has been tested in detail and the number of excitatory (inhibitory) events decreases (increases) as expected with depolarizing (hyperpolarizing) membrane potential values [6]. Moreover, even if EPSPs underestimation happens, only the absolute EPSPs/IPSPs measurements would be affected, but not the normalized comparisons, and thus the relative times of occurrence of both types of events that would remain valid.

In few cases, synaptic activity is detected during down states, predominantly inhibitory activity (Fig. 5d, e, i). In spite of down states being periods of hyperpolarization [7, 35] and excitatory disfacilitation [46], there is some neuronal firing during down states, mostly reported in layer 5 neurons, where up states start. This activity is illustrated in ([35], Fig. 2b), or in ([5], Fig. 1). In [38], it is reported that 43% of the recorded layer 5 neurons have some firing during down states, of an average rate of 3.6 Hz vs. 17.1 Hz during up states. This firing is, according to our model, implicated in the generation of the subsequent up state [5]. The synaptic events reported in Fig. 5d, e, i were obtained from supragranular layers, and thus the inhibitory activity during the down states, which was of 5–20 Hz can be the result of excitatory innervation from layer 5 to inhibitory interneurons in layers 2/3 [9]. Still, such continuous rate of IPSPs was rather unusual. The average rate for down states was 3 and 6 events/s while 37 and 27 events/s (excitatory and inhibitory, respectively) during up states. Up states in vivo revealed an almost identical average rate of events during up states (33 and 31 events/s excitatory and inhibitory, respectively). These numbers are remarkably lower than the ones reported for up states in striatum-cortex-substantia nigra cocultures, which reached a rate of 800 events/s against 10–20 events/s during down states [3].

Activation of excitatory vs. inhibitory neurons during up states in vivo has been reported in [17, 43]. There, the initiation, the initiation, maintenance, and termination of up states in fast to follow network dynamics similar to those in pyramidal cells. Here, we find that the accumulation of excitatory and inhibitory synaptic events is also quite synchronous in vivo as we reported for in vitro. Similar findings were reported in [17], where PSTHs were built with the firing of both excitatory and inhibitory neurons. In our case, we find that the accumulation of synaptic events is 1.4 times faster in vivo than in vitro. We make similar observations if we look at the rise time of the membrane potential, given that the average time for depolarization to the up state is shorter in vivo than in vitro (unpublished observations). The preservation of the thalamocortical loop and of horizontal connections while in vivo can contribute to this faster slope of up states.

Our findings also relate to the debate regarding the relative magnitude of excitatory and inhibitory conductances during the up state. In vitro, we find that inhibitory and synaptic events arrive at a similar rate in the postsynaptic neuron, which could lend support to the balanced conductance observations of Shu et al. [38, 39]. However, we also observed that voltage deflections caused by inhibitory events were almost 4 times larger than those caused by excitatory events, in conditions where driving forces should be approximately equal for both types of events. Then, the overall inhibitory conductance would be larger by a factor 4 than excitatory conductances, as proposed by [33]. In vivo, instead, we did not find a major difference between excitatory and inhibitory synaptic potential amplitudes while we still observed similar rates for inhibitory and excitatory events during up states, in agreement with the results in [17]. Other authors though report larger inhibitory conductances during up states in vivo in average, although approximately half of their recorded neurons showed similar levels of excitatory and inhibitory conductance [34].

Our computational model has allowed us to demonstrate how the precise relationship between excitation and inhibition inputs depends on the structural parameters defining the connectivity in the local cortical circuit. In the light of the large divergence in connectivity parameters for excitatory and inhibitory transmission in the cortex (see "Introduction"), the approximate balance both in timing and magnitude of excitatory and inhibitory synaptic conductances measured experimentally [17, 33, 38, 39] is remarkable and reflects compensation in various of these parameters. By detecting synaptic event timing, rather than synaptic conductance, we can now eliminate one parameter from the equations: the value of excitatory and inhibitory unitary synaptic conductance changes. We find that the number and timing of incoming synaptic events are also approximately matched, so that the unitary synaptic conductances are not the major compensating mechanism for achieving the excitatory–inhibitory balance in the cortex. Instead, our computational model suggests that compensation might be achieved through the tuning of presynaptic firing rate and postsynaptic contacts. Thus, inhibitory interneurons fire at higher rates than pyramidal neurons, and each individual interneuron makes more contacts onto a given postsynaptic neuron [31], so that these factors can balance the fact that pyramidal neurons outnumber inhibitory neurons in the local cortical circuit. However, in light of the caveats of our detection method (section "A Short Discussion on the Method".), we are not in a position of making a strong case in relation with the absolute value of synaptic event rates in the up states.

Instead, the relative timing of excitatory and inhibitory events seems a more robust estimation. Given that pyramidal cortical neurons are known to have a rich local axonal arborization which is typically larger than that of most GABAergic interneurons [23], our experimental finding of a simultaneous arrival of excitatory and inhibitory events is likely to reflect the early firing of inhibitory neurons relative to neighboring excitatory neurons in the transition to the up state, as suggested computationally in [5]. Experimentally, a nonsignificant trend for inhibitory firing leading excitatory firing has been reported in [17,34], but this data generally indicates an activation close to simultaneous for fast spiking and regular spiking neurons. Based on our model simulations, this would indicate an approximately equal horizontal projection length for excitation and inhibition in the cortex, suggesting that intracortical inhibition in the wavefront of the slow oscillation might be principally mediated by the subclass of inhibitory neurons formed by basket cells, which have the longest projection axons among cortical interneurons [24,40]. This prediction can be tested experimentally in the future.

**Acknowledgments** Financial support from Ministerio de Ciencia e Innovación (MICINN) to MVSV and AC is acknowledged. RR was partially supported by the FP7 EU (Synthetic Forager FP7- ICT-217148) and by MICINN.

# Appendix

## Intracellular and Population Recordings In Vitro and In Vivo

### *In Vitro Recordings*

The methods for preparing cortical slices were similar to those described previously [35]. Briefly, 400 μm cortical prefrontal or visual slices were prepared from 3- to 10 month-old ferrets of either sex that were deeply anesthetized. After preparation, slices were placed in an interface-style recording chamber and bathed in ACSF containing (in mM): NaCl, 124; KCl, 2.5; $MgSO_4$, 2; $NaHPO_4$, 1.25; $CaCl_2$, 2; $NaHCO_3$, 26; and dextrose, 10, and was aerated with 95% $O_2$, 5% $CO_2$ to a final pH of 7.4. Bath temperature was maintained at 35–36°C. Intracellular recordings were initiated after 2 h of recovery. In order for spontaneous rhythmic activity to be generated, the solution was switched to "in vivo-like" ACSF containing (in mM): NaCl, 124; KCl, 3.5; $MgSO_4$, 1; $NaHPO_4$, 1.25; $CaCl_2$, 1–1.2; $NaHCO_3$, 26; and dextrose, 10.

### *In Vivo Recordings*

Intracellular recordings in vivo were obtained from rat neocortex (auditory and barrel cortex) as in [32]. Anesthesia was induced by intraperitoneal injection of ketamine (100 mg/kg) and xylacine (8–10 mg/kg) and were not paralyzed. The maintenance dose of ketamine was 75 mg/kg/h. Anesthesia levels were monitored by the recording of low-frequency electroencephalogram (EEG) and the absence of reflexes. Through a craniotomy over the desired area the local field potential was recorded with a tungsten electrode. Intracellular recordings (see below) were obtained in close vicinity from the extracellular recording electrode with identical micropipettes to the ones used to record from the cortical slices.

### *Recordings and Stimulation*

Extracellular multiunit recordings were obtained with 2–4 MΩ tungsten electrodes. The signal was recorded unfiltered at a sampling frequency between 1 and 10 kHz. For intracellular recordings (sampling frequency 10–20 kHz), sharp electrodes of 50–100 MΩ filled with 2 M potassium acetate were used. Sodium channel blocker QX314 (100 μM) was often included in the electrode solution to hold the membrane voltage (Vm) at depolarized potentials while preventing firing.

## Data Analysis and Detection of Synaptic Events

Extracellular recordings were used to identify up and down state onsets. To this end, extracellular recordings were high-pass filtered above 1 Hz to remove slow linear trends in the signal. Then, the envelope of the resulting time series was evaluated as the amplitude of its analytic signal (complex Hilbert transform), high-pass filtered above 0.1 Hz to remove the DC, and smoothed with a running-average square window of 100 ms (Fig. 3). The mean value of this signal was the threshold for the detection of transitions between up state and down state in all recordings. Up states and down states shorter than 250 ms were discarded from the analysis.

Intracellular current clamp recordings were maintained at different membrane voltages by means of current injection. At least two membrane voltages were usually attained: (1) around −70 mV, to achieve chloride reversal potential and isolate EPSPs and (2) around 0 mV, to isolate IPSPs. The timing of presynaptic events of excitatory or inhibitory type were extracted from these intracellular recordings at different membrane voltages (Fig. 3). This was achieved by passing the membrane voltage signal through a differentiator filter with a low-pass cutoff at 200 Hz, thus evaluating a smoothed first time derivative (Fig. 3). This cutoff was not significantly limiting the number of detected synaptic events, as changing it to 500 Hz did not modify our conclusions appreciably. The method has been described in detail in [6]. The timing of synaptic events was detected from sharp voltage deflections in intracellular recordings. Local maxima (minima) are then candidates for excitatory (inhibitory) events, as they represent the fastest voltage upward (downward) deflections in a neighborhood of data points. The central values of these local extremes are typically Gaussian distributed, but extreme values are distributed according to long tails. These long tails presumably contain actual synaptic events, which stick out from noisy membrane voltage fluctuations. To estimate the threshold value that separates these random voltage fluctuations from actual synaptic event voltage deflections, we detected events in the tails of the distribution beyond thresholds set at a fixed number $n$ of interquartile ranges $\sigma$ from the median of the distribution. We used $n$ in the range $n = 2$–$5$, and its precise value was chosen independently for each recorded cell so that more inhibitory events were detected in the depolarized than in the hyperpolarized recording, while at the same time more excitatory events were detected in the hyperpolarized relative to the depolarized recording [6]. For all our analyses here, inhibitory events were extracted just from the depolarized membrane voltage recording and excitatory events just from the hyperpolarized membrane voltage recording.

## References

1. Anderson JS, Carandini M, Ferster D (2000) Orientation tuning of input conductance, excitation, and inhibition in cat primary visual cortex. J Neurophysiol 84:909–926.
2. Bernander O, Koch C, Douglas RJ (1994) Amplification and linearization of distal synaptic input to cortical pyramidal cells. J Neurophysiol 72:2743–2753.

3. Blackwell K, Czubayko U, Plenz D (2003) Quantitative estimate of synaptic inputs to striatal neurons during up and down states in vitro. J Neurosci 23:9123–9132.
4. Borg-Graham LJ, Monier C, Fregnac Y (1998) Visual input evokes transient and strong shunting inhibition in visual cortical neurons. Nature 393:369–373.
5. Compte A, Sanchez-Vives MV, McCormick DA, Wang XJ (2003) Cellular and network mechanisms of slow oscillatory activity (<1 Hz) and wave propagations in a cortical network model. J Neurophysiol 89:2707–2725.
6. Compte A, Reig R, Descalzo VF, Harvey MA, Puccini GD, Sanchez-Vives MV (2008) Spontaneous high-frequency (10–80 Hz) oscillations during up states in the cerebral cortex in vitro. J Neurosci 28:13828–13844.
7. Contreras D, Timofeev I, Steriade M (1996) Mechanisms of long-lasting hyperpolarizations underlying slow sleep oscillations in cat corticothalamic networks. J Physiol 494 (Pt 1): 251–264.
8. Cowan RL, Wilson CJ (1994) Spontaneous firing patterns and axonal projections of single corticostriatal neurons in the rat medial agranular cortex. J Neurophysiol 71:17–32.
9. Dantzker JL, Callaway EM (1998) The development of local, layer-specific visual cortical axons in the absence of extrinsic influences and intrinsic activity. J Neurosci 18:4145–4154.
10. Descalzo VF, Nowak LG, Brumberg JC, McCormick DA, Sanchez-Vives MV (2005) Slow adaptation in fast-spiking neurons of visual cortex. J Neurophysiol 93:1111–1118.
11. Douglas RJ, Martin KA (2004) Neuronal circuits of the neocortex. Annu Rev Neurosci 27:419–451. Review.
12. Erisir A, Lau D, Rudy B, Leonard CS (1999) Function of specific K(+) channels in sustained high-frequency firing of fast-spiking neocortical interneurons. J Neurophysiol 82:2476–2489.
13. Fairen A, DeFelipe J, Regidor J (1984) Non pyramidal neurons: general account. In: Cerebral Cortex (Peters AaJEG, ed.). London: Plenum Press.
14. Feldman ML (1984) Morphology of the neocortical pyramidal neuron. In: Cerebral Cortex (Peters AaJEG, ed.). London: Plenum Press.
15. Galarreta M, Hestrin S (1999) A network of fast-spiking cells in the neocortex connected by electrical synapses. Nature 402:72–75.
16. Gibson JR, Beierlein M, Connors BW (1999) Two networks of electrically coupled inhibitory neurons in neocortex. Nature 402:75–79.
17. Haider B, Duque A, Hasenstaub AR, McCormick DA (2006) Neocortical network activity in vivo is generated through a dynamic balance of excitation and inhibition. J Neurosci 26:4535–4545.
18. Hebb DO (1949) The organization of behavior. New York:Wiley.
19. Kawaguchi Y, Kubota Y (1993) Correlation of physiological subgroupings of nonpyramidal cells with parvalbumin- and calbindinD28k-immunoreactive neurons in layer V of rat frontal cortex. J Neurophysiol 70:387–396.
20. Kruglikov I, Rudy B (2008) Perisomatic GABA release and thalamocortical integration onto neocortical excitatory cells are regulated by neuromodulators. Neuron 58:911–924.
21. Lampl I, Reichova I, Ferster D (1999) Synchronous membrane potential fluctuations in neurons of the cat visual cortex. Neuron 22:361–374.
22. Lorente de Nó R (1938) Analysis of the activity of the chains of internuncial neurons. J Neurophysiol 1:207–244.
23. Lund, JS and Wu, CQ (1997) Local circuit neurons of macaque monkey striate cortex: IV. Neurons of laminae 1–3A. J Comp Neurol 384:109–126.
24. Markram H, Toledo-Rodriguez M, Wang Y, Gupta A, Silberberg G, Wu C (2004) Interneurons of the neocortical inhibitory system. Nat Rev Neurosci 5:793–807.
25. McCormick DA, Connors BW, Lighthall JW, Prince DA (1985) Comparative electrophysiology of pyramidal and sparsely spiny stellate neurons of the neocortex. J Neurophysiol 54:782–806.
26. Megias M, Emri Z, Freund TF, Gulyas AI (2001) Total number and distribution of inhibitory and excitatory synapses on hippocampal CA1 pyramidal cells. Neuroscience 102:527–540.
27. Monier C, Fournier J, Fregnac Y (2008) In vitro and in vivo measures of evoked excitatory and inhibitory conductance dynamics in sensory cortices. J Neurosci Methods 169:323–365.

28. Nowak LG, Azouz R, Sanchez-Vives MV, Gray CM, McCormick DA (2003) Electrophysiological classes of cat primary visual cortical neurons in vivo as revealed by quantitative analyses. J Neurophysiol 89:1541–1566.
29. Okun M, Lampl I (2008) Instantaneous correlation of excitation and inhibition during ongoing and sensory-evoked activities. Nat Neurosci 11:535–537.
30. Pare D, Shink E, Gaudreau H, Destexhe A, Lang EJ (1998) Impact of spontaneous synaptic activity on the resting properties of cat neocortical pyramidal neurons in vivo. J Neurophysiol 79:1450–1460.
31. Peters A (2002) Examining neocortical circuits: some background and facts. J Neurocytol 31:183–193.
32. Reig R, Sanchez-Vives MV (2007) Synaptic transmission and plasticity in an active cortical network. Plos One 2(7):e670.
33. Rudolph M, Pelletier JG, Paré D, Destexhe A (2005) Characterization of synaptic conductances and integrative properties during electrically induced EEG-activated states in neocortical neurons in vivo. J Neurophysiol. Oct 94(4):2805–2821. Epub 2005 Jul 13.
34. Rudolph M, Pospischil M, Timofeev I, Destexhe A (2007) Inhibition determines membrane potential dynamics and controls action potential generation in awake and sleeping cat cortex. J Neurosci 27:5280–5290.
35. Sanchez-Vives MV, McCormick DA (2000) Cellular and network mechanisms of rhythmic recurrent activity in neocortex. Nat Neurosci 3:1027–1034.
36. Schwindt PC, Crill WE (1997) Modification of current transmitted from apical dendrite to soma by blockade of voltage- and $Ca^{2+}$-dependent conductances in rat neocortical pyramidal neurons. J Neurophysiol 78:187–198.
37. Shadlen MN, Newsome WT (1998) The variable discharge of cortical neurons: implications for connectivity, computation, and information coding. J Neurosci 18:3870–3896.
38. Shu Y, Hasenstaub A, McCormick DA (2003a) Turning on and off recurrent balanced cortical activity. Nature 423:288–293.
39. Shu Y, Hasenstaub A, Badoual M, Bal T, McCormick DA (2003b) Barrages of synaptic activity control the gain and sensitivity of cortical neurons. J Neurosci 23:10388–10401.
40. Somogyi P, Kisvarday ZF, Martin KA, Whitteridge D (1983) Synaptic connections of morphologically identified and physiologically characterized large basket cells in the striate cortex of cat. Neuroscience 10:261–294.
41. Steriade M, Nunez A, Amzica F (1993a) A novel slow (<1 Hz) oscillation of neocortical neurons in vivo: depolarizing and hyperpolarizing components. J Neurosci 13:3252–3265.
42. Steriade M, Nunez A, Amzica F (1993b) Intracellular analysis of relations between the slow (< 1 Hz) neocortical oscillation and other sleep rhythms of the electroencephalogram. J Neurosci 13:3266–3283.
43. Steriade M, Timofeev I, Grenier F (2001) Natural waking and sleep states: a view from inside neocortical neurons. J Neurophysiol 85:1969–1985.
44. Stern EA, Kincaid AE, Wilson CJ (1997) Spontaneous subthreshold membrane potential fluctuations and action potential variability of rat corticostriatal and striatal neurons in vivo. J Neurophysiol 77:1697–1715.
45. Thomson AM, West DC, Hahn J, Deuchars J (1996) Single axon IPSPs elicited in pyramidal cells by three classes of interneurones in slices of rat neocortex. J Physiol 496 (Pt 1):81–102.
46. Timofeev I, Grenier F, Steriade M (2001) Disfacilitation and active inhibition in the neocortex during the natural sleep-wake cycle: an intracellular study. Proc Natl Acad Sci U S A 98:1924–1929.
47. Timofeev I, Grenier F, Bazhenov M, Sejnowski TJ, Steriade M (2000) Origin of slow cortical oscillations in deafferented cortical slabs. Cereb Cortex 10:1185–1199.
48. Trevelyan AJ, Watkinson O (2005) Does inhibition balance excitation in neocortex? Prog Biophys Mol Biol 87:109–143.
49. Wang XJ (1999) Synaptic basis of cortical persistent activity: the importance of NMDA receptors to working memory. J Neurosci 19:9587–9603.
50. Wang XJ, Buzsaki G (1996) Gamma oscillation by synaptic inhibition in a hippocampal interneuronal network model. J Neurosci 16:6402–6413.

51. Wehr M, Zador AM (2003) Balanced inhibition underlies tuning and sharpens spike timing in auditory cortex. Nature 426:442–446.
52. Zhu L, Blethyn KL, Cope DW, Tsomaia V, Crunelli V, Hughes SW (2006) Nucleus- and species-specific properties of the slow (<1 Hz) sleep oscillation in thalamocortical neurons. Neuroscience 141:621–636.